Arabian Journal of Chemistry (2018) **11**, 1017–1031

King Saud University

Arabian Journal of Chemistry

www.ksu.edu.sa
www.sciencedirect.com

ORIGINAL ARTICLE

Catalytic effectiveness of azobisisobutyronitrile/[SiMes)Ru(PPH_3)(Ind)Cl_2 initiating system in the polymerization of methyl methacrylate and other vinylic monomers

Abdullah Mohammad Al-Majid [a], Waseem Sharaf Saeed [a], Abdel-Basit Mohammed Al-Odayni [a], Abdulaziz Ali Alghamdi [a], Taieb Aouak [a,*], Fady Nahra [b], Steven Nolan [b]

[a] *Chemistry Department, King Saud University, PO Box 2455, Riyadh 11451, Saudi Arabia*
[b] *Inorganic and Physical Chemistry Department, Ghent University, Krijgslan 281, S-3, 9000 Ghent, Belgium*

Received 23 October 2017; accepted 11 January 2018
Available online 09 February 2018

KEYWORDS

Catalytic effectiveness;
Azobis-isisobutyronitrile/[(SiMes)Ru(PPh_3)(Ind)Cl_2] initiating system;
Living radical;
Polymerization conditions;
Stereo-structure;
Molecular weight distribution;
Kinetics of polymerization

Abstract The catalytic system of azo-bis-isobutyronitrile (AIBN) combined with (SiMes)Ru(PPH_3)(Ind)Cl_2 [M_{20}] was investigated for the controlled radical polymerization of methyl methacrylate (MMA) in solution. Various factors that may influence the catalytic polymerization process, such as the aging time of the initiating system, AIBN/M_{20} ratio, concentration of monomer, polymerization time, temperature, and the nature of solvent were examined. The results showed that the yield, molecular weight, and molecular distribution are practically unaffected by these parameters; however, the syndiotactic stereo-structure tendency that characterizes the produced poly(methyl methacrylate) (PMMA) varied with temperature. The optimum conditions for PMMA synthesis were determined to produce an essentially syndiotactic material with uniformly high molecular weights. It was also revealed that the kinetics of MMA polymerization is of first order with respect to the concentration of monomer. A comparison was also made for some vinylic polymers synthesized either with the AIBN alone or with the AIBN/M_{20}initiating system under the same conditions.

* Corresponding author.
E-mail addresses: amajid@ksu.edu.sa (A. Mohammad Al-Majid), wsaeed@ksu.edu.sa (W.S. Saeed), aalodayni@ksu.edu.sa (A.-B.M Al-Odayni), aalghamdia@ksu.edu.sa (A.A. Alghamdi), taouak@yahoo.fr, taouak@ksu.edu.sa (T. Aouak), Fady.Nahra@UGent.be (F. Nahra), Steven.Nolan@UGent.be (S. Nolan).
Peer review under responsibility of King Saud University.

Production and hosting by Elsevier

https://doi.org/10.1016/j.arabjc.2018.01.006
1878-5352

1. Introduction

In various areas of polymer science and polymer engineering, controlled radical polymerization (CRP) has attracted considerable attention from academia and industry (Matyjaszewski and Xia, 2001; Smirnov, 1990; Smirnov et al., 1981). This emergent technique could overcome certain limitations of the classical radical polymerization process, such as the lack of control over the molecular weight distribution, the end functionalities, and the macromolecular architecture. This polymerization route is efficient and produces well-defined polymers with controlled topology, composition, and functionality (Lin et al., 2009; Xiao et al., 2008; Semsarzadeh and Daronkola, 2006; Kato et al., 1995), which are necessary conditions for a variety of biological and medical applications (Siegwart et al., 2012).

Liu et al. (2015) have copolymerized methyl methacrylate (MMA) with styrene (St) at ambient temperature using sodium hypophosphite ($NaH_2PO_2{\cdot}H_2O$) through a living radical route. This copolymerization reaction proceeded quickly with evident pseudo-first-order kinetics, and linear increase in the molecular weight with increasing monomer conversion and polydispersity index (PDI). Pan et al. (2014) investigated the polymerization of methyl methacrylate in different solvents employed activators generated by electron transfer (AGET ATRP) method. These authors employed $FeCl_3{\cdot}6H_2O$, as catalyst, sodium ascorbate (AsAc-Na) as reducing agent, and the cheap commercial chemical of tetrabutylammonium bromide (TBABR) as ligand. The polymerization in THF showed three advantages compared with that in bulk and in toluene: (1) shortened induction period, (2) enhanced polymerization rate, and (3) better controllability. Bao et al. (2010) successfully synthesized poly(methyl methacrylate) (PMMA) from MMA using two dinuclear cobalt complexes based on bis-diketonate ligands (3,3′-phenylene bis(1-phenylpropane-1,3-di one)and 3,3′-(1,4-phenylene) bis(1-phenylpropane-1,3-dione)) combined with the common initiator of AIBN using the mediated radical polymerization (CMRP) method. The results obtained showed a living polymerization character that displayed linear semi-logarithmic kinetic plots in which the kinetics of this CMRP of MMA were first-order, a linear correlation between the molecular weight and the monomer conversion, and a low PDI. Goto et al. (2008) introduced and developed new family of living radical polymerization using germanium (Ge), tin (Sn), phosphorus (P), and nitrogen (N) catalysts. It was revealed that the polymerization process followed a new reversible activation mechanism and reversible chain transfer catalysis. It was also found that the initiating systems led to narrow molecular weight distribution of homopolymers, random and block copolymers of St, MMA, and functional methacrylates. A new method of producing carbon-centered radicals was discovered by Goto et al. (2013) through a reaction involving an alkyl iodide (R-I) with organic salts to reversibly generate the corresponding alkyl radical (R^*). The organic salts used in this reaction is as a new and a highly efficient organic catalyst in living radical polymerization. The catalytic systems involving tetrabutylammonium iodide and methyltributyl phosphonium iodide were highly reactive. Indeed, these systems permitted the control the polymerization of acrylate and to obtain polymers with high molecular weight, which was difficult to obtain by other organic catalytic systems. Kuroda et al. (2015) investigated the dispersion reversible chain transfer catalyzed polymerization (dispersion RTCP) of MMA in supercritical carbon dioxide ($scCO_2$). These authors demonstrate a RTCP of MMA with 1-phenylethyl iodide (PE-I) as transfer agent and GeI_4 as catalyst in $scCO_2$, where the PE-I is known as non-effective chain transfer agent for polymerization of MAA in RTCP. It was assumed that the reason for the living character in the higher degree of PMMA plasticization by $scCO_2$. These authors advanced the idea to synthesize poly(styrene-block-methylmethacrylate)(PSt-b-PMMA), in which this copolymer is proved difficult to obtain in the homogeneous systems by seeded dispersion RTCP of MMA with PSt-I as macrochain transfer agent and GeI, as catalyst in $scCO_2$. Chen et al. (2004) have successfully carried out the polymerization of MMA by the controlled/"living" radical polymerization route using AIBN/$CuBr_2$/2,2′-bipyridine (bpy)/CH_3CN and AIBN/CuCl/bpy as the initiating system under microwave irradiation (MI). The data revealed that MI enhanced the polymerization rate and also led to a narrower PDI of the resultant PMMA. This system also used a much lower amount of catalyst. MMA and other vinylic monomers have been successively polymerized via ATRP using AIBN/$CuBr_2$/2dNbipy as initiating system by Xia and Matyjaszewski (1997). The obtained PMMA was well-structured and characterized by a low PDI. It was also revealed that high apparent initiation efficiencies for MMA and styrene polymerizations could be achieved at 110 °C. The apparent initiation efficiency decreased and the PDI increased when the [AIBN]/[$CuBr_2$/2dNbipy] ratio was increased. These authors explained the changes in the PDI with respect to the composition of the initiating system by the different deactivation rates by the copper (II) halide species. Bulgakova et al. (2011b) investigated the polymerization of MMA, 2-ethoxyethyl methacrylate and *tert*-butyl methacrylate via CRP in the presence of an AIBN-$FeCl_3{\cdot}6H_2O$-N,N-dimethylformamide initiating system. The rates of all polymerization reactions were first order with respect to the monomer concentration, the molecular weight of the obtained polymers increased linearly with the polymer yield, and their PDI values did not exceed 1.6. The rate of polymerization decreased in the following order: 2-ethoxyethyl methacrylate > MMA > *tert*-butyl methacrylate. The polymerization of MMA in bulk was initiated by $FeCl_3$-$6H_2O$ or $FeCl_3/PPh_3$ at 90 °C without addition of any conventional radical initiator (Bedri et al., 2003). It was concluded in these instances that redox-type reactions were involved in the generation of initiating species. Once the initiating radicals were produced, the reaction occurred via reverse atom-transfer radical polymerization (RATRP). The polymerization reaction was controlled up to a molecular weight of 12,900 g mol^{-1} and polymer yield of 92% using $FeCl_3{\cdot}6H_2O/PPh_3$ initiating system.

We have been interested in this transformation for some time, and are also intrigued by the possibility of other metal centers enabling this transformation. Ruthenium–indenylidene complexes are generally known as very efficient promoters of olefin metathesis and are most prevalently used in ring-closing metathesis reaction (Le et al., 2013, Monsaert et al., 2010, De Frëmont et al., 2008, Dragutan et al., 2005, Jafarpour et al., 1999). However, the use of these complexes as initiating systems in CRP technique is relatively recent. They have been used to polymerize a large number of vinylic monomers, such as acrylates, methacrylates, and St; and are

continuously developed. Simal et al. (2000) used a series of ruthenium-based catalytic systems to polymerize MMA and St via the ATRP method. Their results revealed that only [$RuCl_2$(p-cymene) (PR_3)] complexes bearing both strongly basic and bulky ligands (such as P(i-Pr)$_3$, P(cyclohexyl)$_2$Ph, P (cyclohexyl)$_3$, and P(cyclopentyl)$_3$), were efficient catalysts for the ATRP of these monomers. De Clercq and Verpoort (2003) examined the ATRP of vinyl monomers mediated by a class of ruthenium alkylidene catalyst systems containing 1, 3-dimesityl-4,5-dihydroimidazol-2-ylidene (SIMes) combined with a Schiff base as ligand. Under biphasic conditions (organic/aqueous), cationic analogues of these systems produce PMMA and polystyrene (PSt) with narrow molecular weight distribution through a radical polymerization mechanism. Kato et al. (1995) reported a living polymerization of MMA initiated by carbon tetrachloride, dichlorotris(triphenyl phosphine)ruthenium(II)[$RuCl_2(PPh_3)_3$], and methylaluminum bis(2,6-di-*tert*-butylphonoxide)[MeAl-($ODBPO_2$] system. The polymerization process appeared to be follows a radical route that involves a reversible and homolytic cleavage of the carbon-halogen terminal assisted by the transition metal complex. The ruthenium(II) complex interacts with CCl_4 as initiator to be oxidized from divalent to trivalent followed by the radical addition of CCl_3^* to MMA, and then ruthenium(III) species formed is then reduced to the original ruthenium(II) complex leading to the CCl_4-MMA adduct containing a terminal C—Cl bond. The polymerization occurred according to similar repetitive addition of MMA to the radical species with the C—Cl terminal. Analogue approach in the control radical polymerization has also reported by Wang and Matyjaszewski (1995). Ando et al. (1996) developed ruthenium-based living radical polymerization of MMA using alternative initiators obtained by the replacement of CCL_4 or $MeAl(ODBP)_2$ by aluminum compounds used by Mitsuru et al. in the previous investigation. These authors employed α-halocarbonyl compounds as potent initiators. So that the structures simulate the polymer terminal group linked to the same atom of carbon. It was revealed from the results obtained that the living polymerization of MMA could be achieved using this initiator system in which a conversion of more 90% was reached during 60–80 h and the polymers obtained have PDI inferior to 1.2 smaller than those obtained when the $ClCl_4$ is employed. From this investigation, it was also revealed that the average molecular number directly increased with monomer conversion. In this present study, the polymerization of MMA using AIBN combined with [(SIMes)Ru (PPh_3)(Ind)Cl_2][M_{20}] (Scheme 1) was explored systematically for the first time. We determined the optimum conditions to produce PMMA with lower PDI, higher syndiotactic stereostructure, and relatively high molecular weights compared with those reported using other CRP catalytic systems. To reach this goal, the [AIBN]/[M_{20}] ratio, concentration of monomer, time, solvent, and the temperature of polymerization were varied and correlated to the properties of the generated polymers.

Preliminary studies have shown that well-defined PMMA could be obtained using the simple AIBN/M_{20} as initiating system (Al-Majid et al., 2017). A series of vinylic monomers was also polymerized in presence of this system under the obtained optimum conditions. The results obtained were compared with those from the traditional route using AIBN alone as initiator.

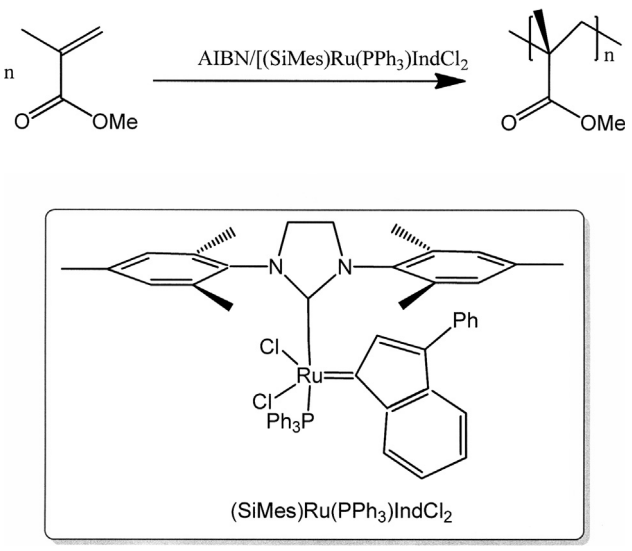

Scheme 1 Polymerization reaction of MMA using AIBN/M_{20} initiating system.

After describing the polymerization of MMA in detail, we applied the optimum conditions to the reactions of other monomers.

2. Materials and methods

2.1. Materials

MMA, ethyl methacrylate (EMA), *n*-butyl methacrylate (BMA), methacrylic acid (MAA), Acrylamide (AM) and St (Sigma Aldrich, superior to 98% purity) were purified by vapor condensation in a cold-walled trap containing dehydrated $CaCl_2$. 1,4-dioxane, 2-butanone, chloroform, and toluene (Fluka, 99% purity). They were distilled under nitrogen in the presence of the same desiccant and collected as the monomer in a flask containing molecular sieve. AIBN (Aldrich, 98% purity) was purified several times by recrystallization in methanol. *[Ru(ind)(SIMes)(PPh_3Cl_2)] (M_{20})* synthesized as described below and used without further purification.

2.2. Synthesis of [Ru(ind)(SIMes)(PPh_3Cl_2)] (M_{20})

M_{20} was synthesized according to the procedure described in the literature (Al-Majid et al., 2017). In the glove box, *[RuCl (PPh_3)$_2$(Ind)]* (M_{10}) (1.00 g, 1.13 mmol) and the NHC (SIMes, 366 mg, 1.18 mmol) were charged into a Schlenk flask and dissolved in toluene (3 mL). The reaction mixture was taken out of the glove box and stirred at 40 °C for 3 h under Argon. Afterwards, the mixture was allowed to cool to RT, and hexane (30 mL) was added to precipitate the product, the suspension was cooled to −40 °C. Filtration and washing with cold methanol (1 × 4 mL) and cold hexane (4 × 10 mL) afforded M_{20}(920 mg, 88%) as microcrystalline solid. Analytical data are as reported in the literature (Al-Majid et al., 2017).

2.3. Polymerization

All polymerization reactions were performed in 1,4-dioxane under an inert atmosphere of nitrogen in a reactor as reported by Al-Majid et al. (2017). After the desired reaction time, the resulting polymer was isolated by precipitation, washing in methanol containing 5 wt% of hydrochloric acid, and then dried at 50 °C under vacuum for 24 h. The polymer films were prepared by smoothly casting the mixed solution of polymer and residual monomer in 1,4-dioxane over a Teflon plate surface. The plate was then heated at 40 °C for 24 h and dried under vacuum at 50 °C for another 24 h. The average thickness of the resulted films ranged from 123 to 188 μm.

2.4. Analysis

The molecular mass of the prepared polymers was measured in THF at 30 °C by size exclusion chromatography (SEC) on a Varian apparatus equipped with a JASCO type 880-PU HPLC pump, refractive index and UV detectors and TSK Gel columns calibrated with PSt standards. The FTIR spectra of polymers were recorded on a Perkin Elmer 1000 spectrophotometer at room temperature. In all cases, at least 32 scans with an accuracy of 2 cm^{-1} were signal-averaged. The film samples were transparent and sufficiently thin to obey the Beer Lambert law. The structure and microstructure of the polymers were determined quantitatively in THF-d_8 by ^1H and ^{13}C NMR spectroscopy using a JEOL FX 90 Q NMR instrument at 500 and 200 MHz, respectively. DSC thermograms of polymers were recorded on a Shimadsu DSC 60 system previously calibrated with indium. The polymer film (8–10 mg) film was packed in aluminum DSC pans before placing in DSC cell. The sample was then heated from −50 to 250 °C at a heating rate of 10 °C min^{-1}.

3. Results and discussion

3.1. Characterization

The FTIR spectrum confirmed the complete disappearance of the absorption band of vinylic group (C═C) of MMA at 1624 cm^{-1}. The ^1H NMR spectrum showed the disappearance of both signals at 6.25 ppm and 5.70 ppm which are assigned to the two geminal protons of the vinylic group. The ^{13}C NMR spectrum revealed the total absence of signals at 136.22 ppm and 125.34 ppm attributed to the substituted and unsubstituted carbon of the monomer, respectively. As shown in Fig. 1, the stereo-structure of PMMA was determined by ^1H NMR method through the deconvolution of the broad peak localized between 1.10 and 2.15 ppm. The deconvoluted peaks at 1.90, 1.85 and 1.77 ppm were assigned to Hβ (*mrr*), Hβ (*rrr*) and CH_2 (*r*), respectively.

The results showed predominant syndiotactic stereo-structure (61–78%) depending on the experimental conditions. This result seems to be higher compared to that from the literature: a maximum of 69% of syndiotactic stero-structure (Hiraki et al., 1971) using a catalyst system derived from dichloro (dodeca-2,6-triene-1,12—diyil) ruthenium (IV) and triphenylphosphine, 55–61% using a modified traditional microemulsion polymerization (Jiang et al., 2004) and 48%

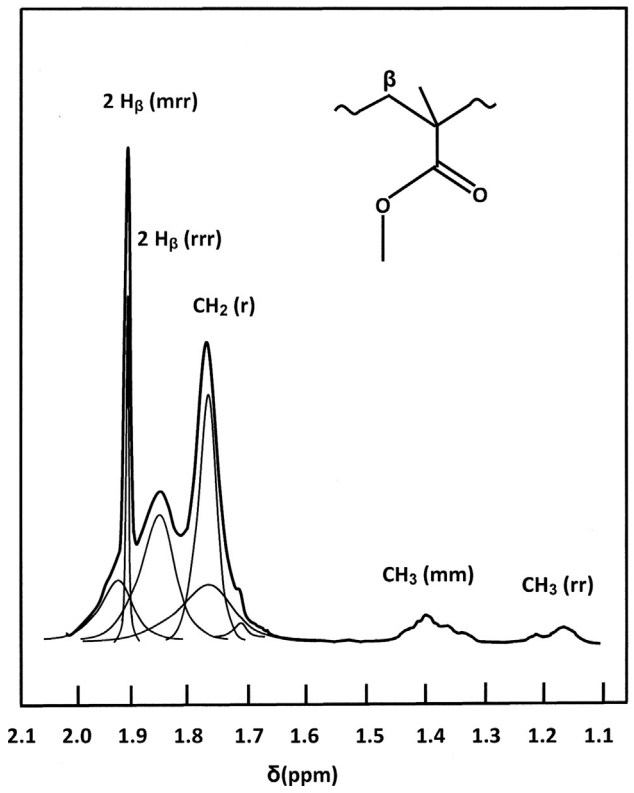

Fig. 1 Deconvolution of the ^1H NMR spectrum (1.10–2.15 ppm) of PMMA via Lorentzian peaks.

commercial PMMA (Hiraki et al., 1971; Thompson, 1966). The average molecular weight of PMMA determined by the SEC method was relatively high (0.27×10^5–3.60×10^5 g mol^{-1}) and characterized by a narrow molecular distribution, in which the DPI (D stroke) varied between 1.10 and 1.62. To highlight the character of the radical polymerization control of the AIBN/M_{20} initiating system, the average molecular weight of the obtained polymers was compared with that obtained by a simple calculation from the polymer yield using the following equation

$$M_n^{cal} = \frac{yield \times N \times M_m}{100 \times N_{fr} \times f} \quad (1)$$

f is the efficient factor which is determined from the equation below

$$f = \frac{M_n^{cal}}{\overline{M}_n^{exp}} \quad (2)$$

where N, N_{fr} and M_m are the mole number of monomer, number of free radical resulted from the dissociation of AIBN (i.e., (2)) and the molar mass of monomer, respectively.

The tacticity of PMMA was determined by ^1H NMR spectroscopy based on the chemical shift of the 2Hβ protons localized at 1.77, 1.85 and 1,91 ppm, which are assigned to the 2Hβ(mrr), 2Hβ(rrr) tetrads and CH_2(r) dyads, respectively (Al-Majid et al., 2017). Basing on the integration of each signal from the deconvoluting the broad signals localized between 1.62 and 2.07 ppm via Lorentzian peaks, it was possible to easily evaluate the tacticity of each PMMA (aliphatic CH, 1.10–2.15 ppm) and that of the three protons in PMMA

(α-methyl group, 1.62–2.07 ppm). Noting that, to approach the exact value of the tacticity percentage, the mother peak must be the most possible covered by the total sum of these derivative peaks. The predominantly syndiotactic microstructure is probably due to the fact that when MMA monomer is added to the PMAA radical during the propagation step, a marked preference is observed for the new chiral center to adopt a configuration opposite to that of the preceding (penultimate) unit in the chain (Moad et al., 1986. In this way, the substituent-substituent electrostatic repulsions are favorable in this surrounding forcing the macromolecules to take a more stable conformation as in the syndiotactic triads. This syndiotactic preference diminished with increasing the temperature as observed in the Section 3.3.

Fig. 2 compares the DSC thermograms of PMMA with comparable molecular weights, synthesized by the AIBN/M_{20} system in different conditions, and that obtained by AIBN alone. The curves show that the range of glass transition time of PMMA obtained by the combined system is about three times shorter compared with that obtained with AIBN alone (from 8 to 22 min) and increases with DPI. The data also revealed that the glass transition temperature, T_g, also shifted toward the low temperature (from122 to 116 °C) when the DPI was increased. It is well known that the T_g of a polymer depends within a certain limit on its molecular weight (Fox and Flory, 1950, Beevers and White, 1960, Blanchard et al., 1974, Agapov and Sokolov, 2009). Therefore, the T_g in the case of a wide molecular weight distribution in the polydisperse polymer is a result of several successive T_g. The shift in the T_g value toward the low temperatures observed for the polydisperse PMMA synthesized by AIBN alone is probably

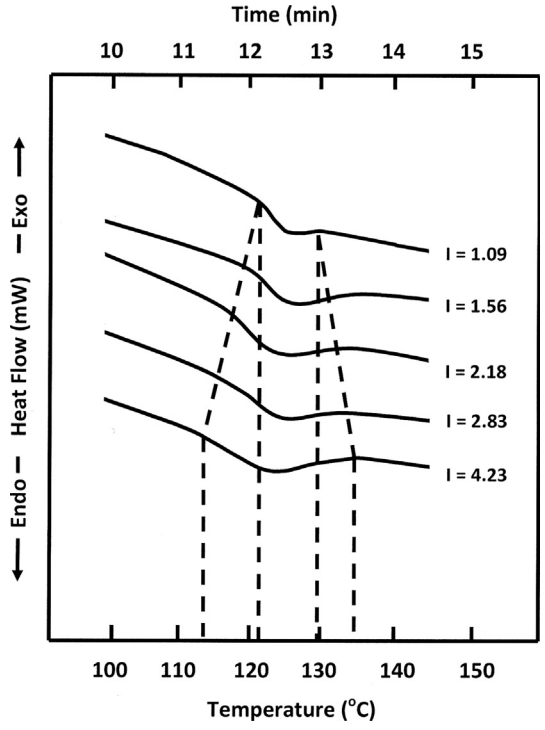

Fig. 2 DSC thermograms of PMMA synthesized by the AIBN/M_{20} initiating system in different conditions obtaining under gas nitrogen at a heating rate of 10 °C min^{-1}.

due to the polymer chain portions with low molecular weights, which play the role of plasticizer facilitating the chains sliding against each other. Similar results were also observed by Blanchard et al., 1974 by comparing the T_g of PSt monodisperse and polydisperse polystyrene samples

3.2. Effect of the initiator system aging time

The aging process is necessary for testing an initiator system to know if the initiator (AIBN) reacts with the monomer independently of the co-initiator (M_{20}), in this case, the results of the polymerization are not affected by the aging time, or reacts with the co-initiator leading to the formation of new initiating species leading to different polymerization results. The influence of aging time of the initiating system on the polymerization of MMA was examined in 1,4 dioxane at 70 °C at time ranged between 5 and 120 min prior to add the monomer and the results obtained are grouped in Table 1. The data obtained, indicate that the experimental average molecular weights obtained during 6 h of the polymerization process agrees well with those calculated from Eq. (1). It was also found that the yield and the average molecular weight decreased with increasing the aging time, while the DPI remained nearly constant (1.09–1.17). The decrease in the yield and the molecular weight versus time clearly indicates that aging time does not work well in the M_{20}/AIBN combination. This finding seems also indicates a deactivation process of the initiating species number was occurred during the aging time. Indeed, we can know conclude from these results obtained that the polymerization process seems initiated by initiator species resulted from the combination of AIBN with M_{20} and not independently.

The apparent stability of the PDI indicates that there was a dramatic reduction of the transfer reactions from the beginning of the addition of M_{20} to the AIBN. The influence of the aging time on the tacticity of PMMA (determined by ^{1}-HNMR) is presented in Table 2. All obtained PMMA samples have a fairly constant preference for syndiotactic structure (~73%). This finding indicates that the successive insertion of monomer in the growing chain is unaffected by the aging time.

3.3. Effect of the concentration of MMA

The effect of the MMA concentration on the polymerization at 70 °C during 6 h is shown in Table 3. The polymer yield and the average molecular weight decrease as the concentration of monomer increases. On the other hand, the molecular weight distribution remains practically constant, as long as the concentration of monomer does not exceed 4.68 mol L^{-1}, then dramatically increased to reach 2.83 when 8.0 mol L^{-1} of monomer was added. In our case, the decrease of the polymerization yield with increasing the concentration of monomer seems to be complex to rigorously explain because of the complexity of the initiating system used and the absence of supplementary analysis used to highlight certain points. To have an idea on the complexity of this initiator system it is sufficient to analyze the results obtained with changing the aging time in Section 3.1. However, we can always anticipate and attribute this fact to the increase of the viscosity of the reaction mixture due to the increase of the molecular weight leading

Table 1 Variation of the yield, molecular weight and the PDI versus the aging time of the AIBN/M_{20} initiating system.

Experiment	Aging time (min)	Yield (%)	$\overline{M}_n \times 10^{-5}$ (g mol^{-1})	$\overline{M}_w \times 10^{-5}$ (g mol^{-1})	$\overline{M}_{cal} \times 10^{-5}$ (g mol^{-1})	$\frac{\overline{M}_w}{\overline{M}_n}$	f
1	5	78.23	1.43	1.56	1.50	1.09	1.04
2	25	59.53	1.08	1.21	1.14	1.12	1.03
3	30	52.25	0.96	1.08	1.03	1.12	0.93
4	60	40.90	0.77	0.85	0.79	1.11	0.97
5	120	38.86	0.72	1.01	0.75	1.17	0.96

Experimental conditions: solvent: 1,4-dioxane; aging temperature: 70 °C; polymerization time: 6 h; polymerization temperature: 70 °C; [MMA] = 2.35 g (4.68 mol L^{-1}); [AIBN] = 1.0 mg ($1.22 \cdot 10^{-3}$ mol L^{-1}); [AIBN]/[Ru] = 1.0.

Table 2 Effect of the aging time on the tacticity of PMMA.

Experiment	Aging time (min)	Triad tacticity (%)		
		mm	*mr*	*rr*
1	5	4	23	73
2	25	7	21	72
3	30	6	22	73
4	60	7	20	73
5	120	3	25	72

Experimental conditions: Solvent: 1,4-dioxane; Aging temperature: 70 °C; polymerization time: 6 h; polymerization temperature: 70 °C; [MMA] = 2.35 g (4.68 mol L^{-1}); [AIBN] = 1.0 mg ($1.22 \cdot 10^{-3}$ mol L^{-1}); [AIBN]/[Ru] = 1.0.

Table 3 Effect of the concentration of MMA on the polymer yield, molecular weight and polydispersity index.

Experiment	[MMA] (mol L^{-1})	Yield (%)	$\overline{M}_n$ ($\times 10^{-5}$) (g mol^{-1})	$\overline{M}_w$ ($\times 10^{-5}$) (g mol^{-1})	$\overline{M}_{cal}$ ($\times 10^{-5}$) (g mol^{-1})	$\frac{\overline{M}_w}{\overline{M}_n}$	*f*
1	1.50	95.62	0.54	0.59	0.58	1.10	1.07
2	2.35	82.57	0.75	0.83	0.80	1.11	1.06
3	4.68	78.23	1.43	1.56	1.50	1.09	1.05
4	6.00	67.17	1.56	3.40	1.65	2.18	1.06
5	8.00	60.34	1.81	5.12	1.98	2.83	1.09

Experimental conditions: solvent: 1,4-dioxane; aging temperature: 70 °C; aging time: 5 min; polymerization time: 6 h; polymerization temperature: 70 °C [AIBN] = 0.1 mg ($1.22 \cdot 10^{-3}$ mol L^{-1}); [AIBN]/[Ru] = 1.

Table 4 Effect of the monomer concentration on the PMMA tacticity.

Experiment	[MMA] (mol L^{-1})	Triad tacticity (%)		
		mm	*mr*	*rr*
1	1.50	2	24	74
2	2.35	4	23	73
3	4.68	4	23	73
4	6.00	5	22	73
5	8.00	4	23	73

Experimental conditions: solvent: 1,4-dioxane; aging temperature: 70 °C; aging time: 5 min; polymerization time: 6 h; polymerization temperature: 70 °C; [AIBN] = 0.1 mg ($1.22 \cdot 10^{-3}$ mol L^{-1}); [AIBN]/[Ru] = 1.

to a dramatically decrease of the polymerization kinetic. According to the results provided in Table 4, the PMMA tacticity is virtually unaffected by the monomer concentration.

3.4. Influence of [AIBN]/M_{20} molar ratio

The effect of the [AIBN]/[M_{20}] ratio on the polymerization results is illustrated in Table 5 and plotted in Fig. 3. As shown from these curve profiles, the polymer yield increased and passed by a pseudo plateau between 50 and 70%. The profiles of the SEC chromatograms of the PMMA obtained are grouped in Fig. 4 and the molecular weights, obtained at different [AIBN]/[M_{20}] ratio are deducted from the calibration curve and an example of the data treated is presented in Fig. 5. As can be seen from the curve profiles of Fig. 3, the average molecular weight versus the [AIBN]/[M_{20}] ratio increased discontinuously with increasing the [AIBN]/[M_{20}] ratio. Indeed, the average molecular weight in the same per-

Table 5 Variation of the polymerization yield, molecular weight and polydisperisity index versus the [AIBN]/[M_{20}] ratio.

Experiment	*[AIBN]/[M$_{20}$]* mol(%)	*Yield* (wt%)	$\overline{M}_n$ ($\times 10^{-5}$) (g mol^{-1})	$\overline{M}_w$ ($\times 10^{-5}$) (g mol^{-1})	$\overline{M}_{cal}$ ($\times 10^{-5}$) (g mol^{-1})	$\frac{\overline{M}_w}{\overline{M}_n}$	*f*
1	10:90	57.10	1.12	1.21	1.09	1.08	0.97
2	25:75	66.56	1.32	1.44	1.28	1.09	0.97
3	50:50	78.23	1.43	1.55	1.50	1.09	1.05
4	75:25	82.32	3.36	4.56	1.58	1.36	0.47
5	90:10	90.78	3.48	9.67	1.74	2.78	0.50
6	100:0	97.12	5.12	21.66	1.86	4.23	0.36

Experimental conditions: solvent: 1,4-dioxane; aging temperature: 70 °C; aging time: 5 min; polymerization time: 6 h; polymerization temperature: 70 °C; [AIBN] = 0.1 mg L^{-1} ($1.22 \cdot 10^{-3}$ mol L^{-1}); [MMA] = 2.35 g (4.68 mol L^{-1}).

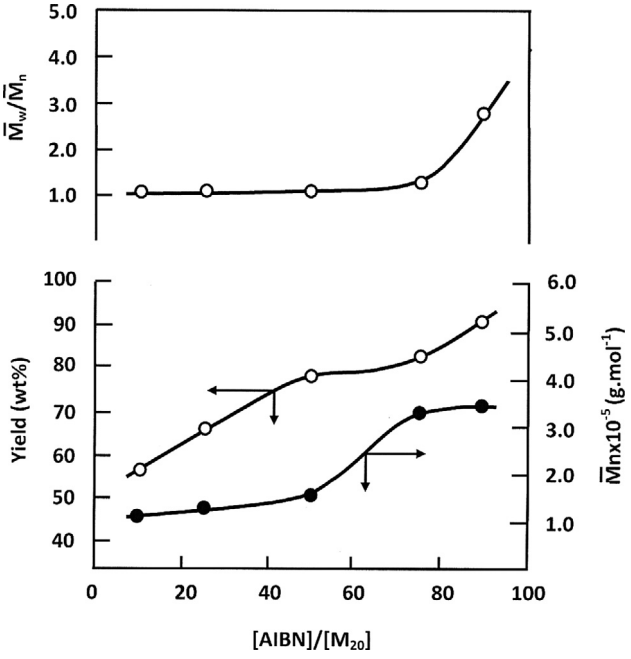

Fig. 3 Variation of the yield, average molecular weight and $\overline{M}_w/\overline{M}_n$ of PMMA versus [AIBN]/M_{20} ratio. The experimental conditions were: solvent: 1,4-dioxane; aging temperature: 70 °C; aging time: 5 min; polymerization time: 6 h; polymerization temperature: 70 °C; [AIBN] = 0.1 mg L^{-1} ($1.22 \cdot 10^{-3}$ mol L^{-1}); [MMA] = 2.35 g (4.68 mol L^{-1}).

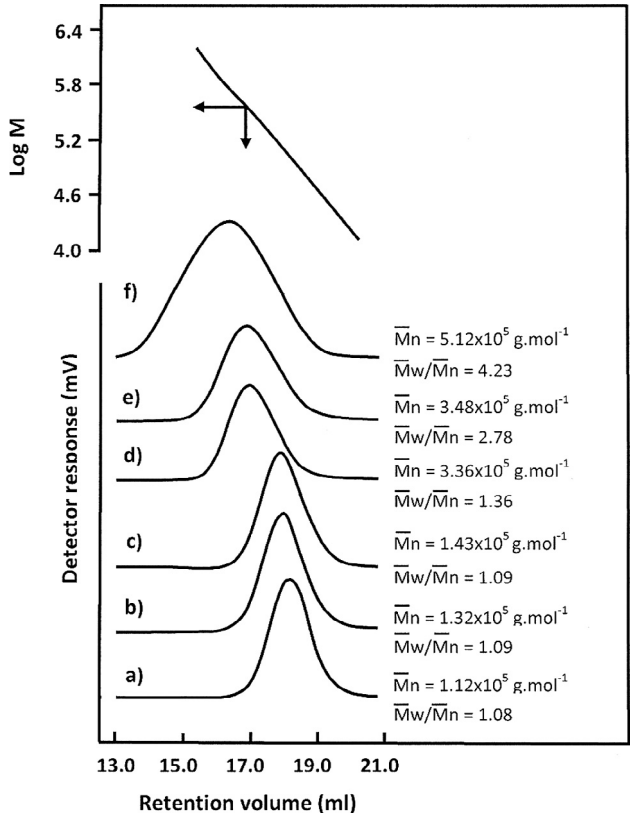

Fig. 4 SEC chromatograms of PMMA synthesized at 70 °C with different [AIBN]/[M_{20}] ratio: (a) 10:90; (b) 25:75; (c); 50:50; (d) 75:25; (e) 90:10 and (f) 100:0 mol ratio. The experimental conditions were: solvent: 1,4-dioxane; aging temperature: 70 °C; aging time: 5 min; polymerization time: 6 h; polymerization temperature: 70 °C; [AIBN] = 0.1 mg L^{-1} ($1.22 \cdot 10^{-3}$ mol L^{-1}); [MMA] = 2.35 g (4.68 mol L^{-1}).

centage range passed by an inflexion between 50 and 70% in which its value dramatically increased. However, as shown in the up of this same figure, the molecular weight distribution remains practically unchanged between 10 and 70 mol% and dramatically linearly increases (1.36–4.23) with increasing the [AIBN]/[M_{20}] ratio.

"Effect [AIBN]:[M20]. For high ratios the aspect of two type of polymers: (i) controlled (CRP) and (ii) conventional like is mentioned.

The discontinuity in the variation of the yield versus the PDI, and the molecular weight versus the composition of initiating system clearly suggest the presence of two simultaneous modes of initiation. The polymerization of MMA with [AIBN]/[M_{20}] ratio < 70 mol% is initiated by AIBN combined with M_{20} complex, leading to well-defined polymer through a controlled pure radical polymerization route. In contrast, that with [AIBN]/[M_{20}] ratio superior to 70 mol% appears to be initiated by two separate active species. Indeed, the product consists of two polymer types, one is a well-defined PMMA (PDI ≈ 1.08–1.09) produced by the active centers involving AIBN combined with M_{20} via a CRP route, the other is characterized by wide molecular weight distributions (2.36–4.23) and relatively high molecular weights because it is produced by the active centers involving only the residual AIBN via a traditional polymerization route. This finding confirms those of the CRP reported in the literature (D'Hooge et al., 2012) and explains the discrepancy between

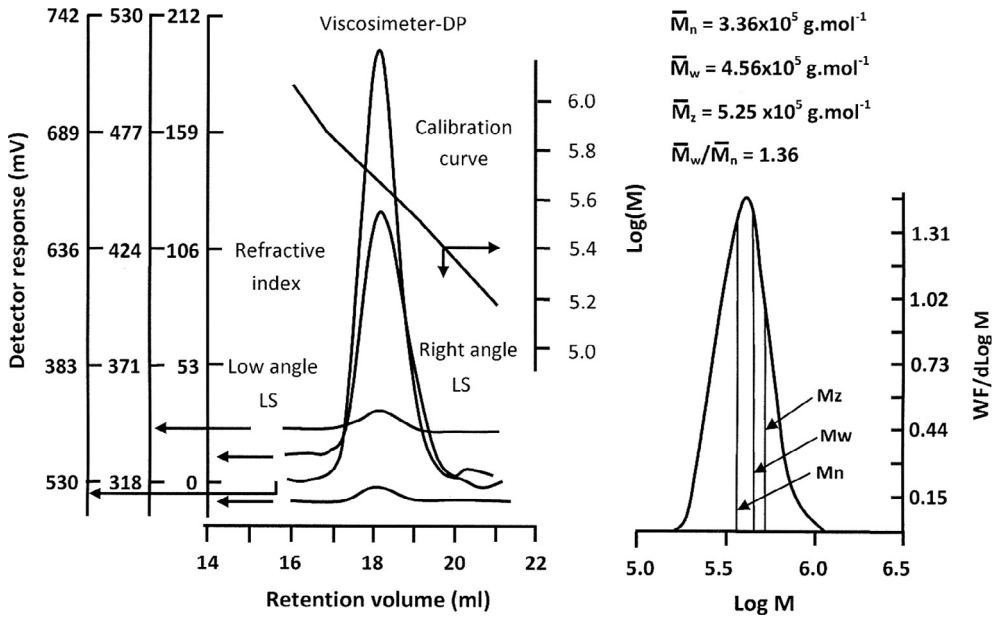

Fig. 5 SEC Chromatogram of PMMA synthesized in the experimental conditions: solvent: 1,4-dioxane; aging temperature: 70 °C; aging time: 5 min; polymerization time: 6 h; polymerization temperature: 70 °C; [AIBN] = 0.1 mg L^{-1} ($1.22 \cdot 10^{-3}$ mol L^{-1}); [AIBN]/[M_{20}] = 75:25; [MMA] = 2.35 g (4.68 mol L^{-1}).

Table 6 Effect of the [AIBN]/[M_{20}] ratio on the PMMA tacticity.

Experiment	[AIBN]/[M_{20}] (mol/mol)	Triad tacticity (%)		
		mm	*mr*	*rr*
2	10:90	3	22	75
3	25:75	3	23	74
4	50:50	4	23	73
5	75:25	2	25	73
6	90:10	3	26	71
7	100:0	5	27	68

Experimental conditions: solvent: 1,4-dioxane; aging temperature: 70 °C; aging time: 5 min; polymerization time: 6 h; polymerization temperature: 70 °C; [AIBN] = 0.1 mg L^{-1} ($1.22 \cdot 10^{-3}$ mol L^{-1}); [MMA] = 2.35 g (4.68 mol L^{-1}).

Table 7 Effect of the polymerization time on the PMMA yield, molecular weight and polydispersity index of the polymer produced.

Experiment	Time (h)	Yield (%)	$\overline{M}_n$ ($\times 10^{-5}$) (g mol^{-1})	$\overline{M}_w$ ($\times 10^{-5}$) (g mol^{-1})	$\overline{M}_{cal}$ ($\times 10^{-5}$) (g mol^{-1})	$\frac{\overline{M}_w}{\overline{M}_n}$	*f*
1	0.5	12.71	0.27	0.29	0.24	1.08	0.88
2	1.0	14.57	0.30	0.33	0.28	1.10	0.93
3	2.0	34.03	0.60	0.65	0.65	1.09	1.08
4	4.0	52.24	0.94	1.05	1.00	1.12	1.06
5	6.0	78.23	1.43	1.56	1.50	1.09	1.05

Experimental conditions: Solvent: 1,4-dioxane; aging temperature: 70 °C; aging time: 5 min; [AIBN]/[Ru] = 1; [AIBN] = 0.1 mg L^{-1} ($1.22 \cdot 10^{-3}$ mol L^{-1}); [MMA] = 2.35 g (4.68 mol L^{-1}); polymerization temperature: 70 °C.

the experimental and calculated values of the molecular weights ($\overline{M}_n$ and M^{cal}, respectively). This study shows that this initiating system has the best performance when AIBN and M_{20} were in equal concentration. The variation of the syndiotactic stereo-structure of PMMA versus [AIBN]/M_{20} ratio is presented in Table 6 and the results reveal that the syndiotactic stereo-structure slowly decreased when the AIBN/M_{20} ratio increased. This finding seems to indicate that when the AIBN/M_{20} ratio is $\geq$50 mol%, the monomer is preferentially incorporated alternatively on the macro-radical in progression. On the other hand, when the AIBN/M_{20} ratio is $>$50 mol%, the syndiotactic stereo-structure of the PMMA seems to be

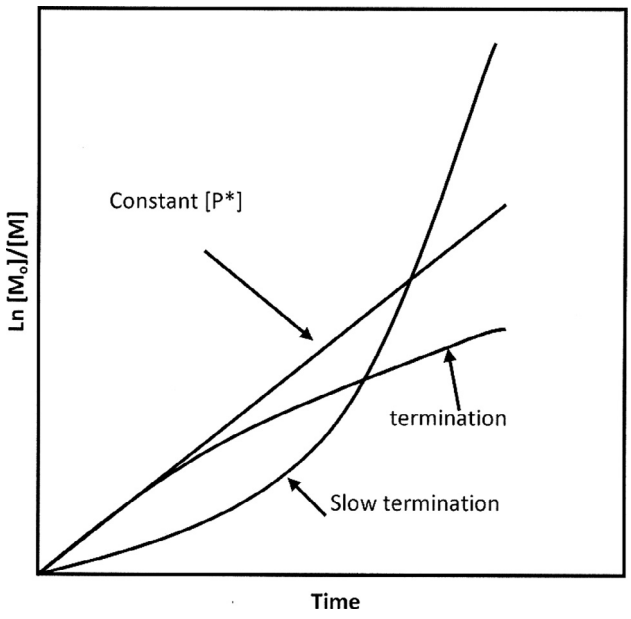

Scheme 2 Dependence of Ln([M]$_o$/[M]) on time.

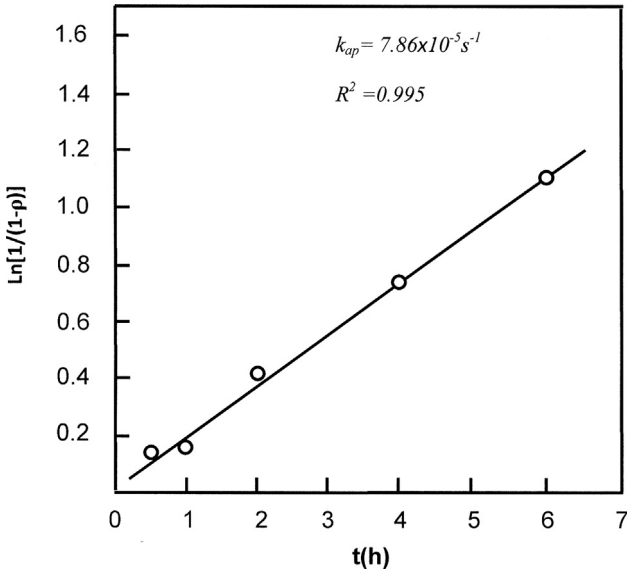

Fig. 6 Time dependence of $Ln[1/(1-\rho)]$ for the polymerization of MMA in 1,4-doxane. The experimental conditions were: Solvent:1,4-dioxane; aging temperature: 70 °C; aging time: 5 min; [AIBN]/[Ru] = 1; [AIBN] = 0.1 mg L^{-1} ($1.22 \cdot 10^{-3}$ mol L^{-1}); [MMA] = 2.35 g (4.68 mol L^{-1}); polymerization time: 6 h.

produced via two competiting initiating systems: a portion of the PMMA mixture has syndiotactic stereo-structure of 68% initiating by residual AIBN alone, and another portion from the AIBN combined with M_{20} complex leading to a 73% syndiotactic PMMA.

3.5. Influence of the polymerization time

The analytical data presented in Table 7 show the influence of the reaction time on the on the polymerization of MMA involving the AIBN/M_{20} initiating system in 1,4-dioxane. Both the yield and molecular weight increased with the polymerization time, while there is no change in the PDI. Noting that, for comparable time and temperature using the traditional free radical polymerization initiated by AIBN, the polymer yield, average number molecular weight, average weight molecular weight and PDI were 93 wt%, $4.7 \cdot 10^5$ g mol^{-1}, 1.84 g mol^{-1} and 3.94, respectively.

The predominantly syndiotactic stereo-structure of PMMA remains unaffected during the polymerization time. This finding also indicates that the change in viscosity of the polymeric solution during the reaction does not affect the microstructure of the resulting polymer.

According to Arslan (2012), in general, in a CRP it is widely accepted that the controlled polymerization process should display four principal features: the first order kinetic behavior, pre-determinable degree of polymerization, designed narrow molecular weight distribution and long-lived polymer chain with preserved end functionalities. The rate of polymerization, R_p, concerning the logarithm of the monomer concentration vary linearly with time. This linearity is usually due to the negligible contribution of no-reversible termination, so that the concentration of the active propagating species remains constant during the polymerization.

$$R_p = \frac{-d[M]}{dt} = K_p[R^*][M] \tag{3}$$

were [M] and [R*] are the concentrations of monomer and active propagating species. K_p is the constant of propagation.

$$Ln\frac{[M]_o}{[M]} = K_p[R^*]t = K_p^{app}t \quad \text{(this is possible if } [R^*] = \text{constant)} \tag{4}$$

$$Ln\frac{1}{1-\rho} = K_p^{app}t \tag{5}$$

where $[M]_o$ and $[M]$ are the initial and final concentrations of monomer none polymerized.

K_p^{app} is the apparent constant of propagation and ρ the polymer yield reached at t of the reaction process. This ρ value is calculated from the following Eq. (6)

$$\rho = 1 - \frac{[M]}{[M_o]} \tag{6}$$

Three possibilities may be presented from Eq. (3) according to the effect of changes in R* as illustrated in Scheme 2. These curve profiles indicate the logarithmic plot is very sensitive to any change in the concentration of the active propagating species. Indeed, a constant [R*] a straight line is revealed. A steady [R*] in a CRP is established by balancing the rates of activation and deactivation and not by balancing the rates of initiation and termination as the case of a conventional radical polymerization. An upward curvature in this plot reveals an increase in [R*], which is observed in the case of slow initiation. However, a downward curvature indicated a decrease in [R*], which can result from the termination reactions increasing the concentration of the persistent radical, or some other side reactions such as the catalytic system being poisoned or redox processes on the radical. Noting that, the logarithmic plot is not sensitive to chain transfer processes or slow exchange between different active species, since they do not affect the number of the active propagating species.

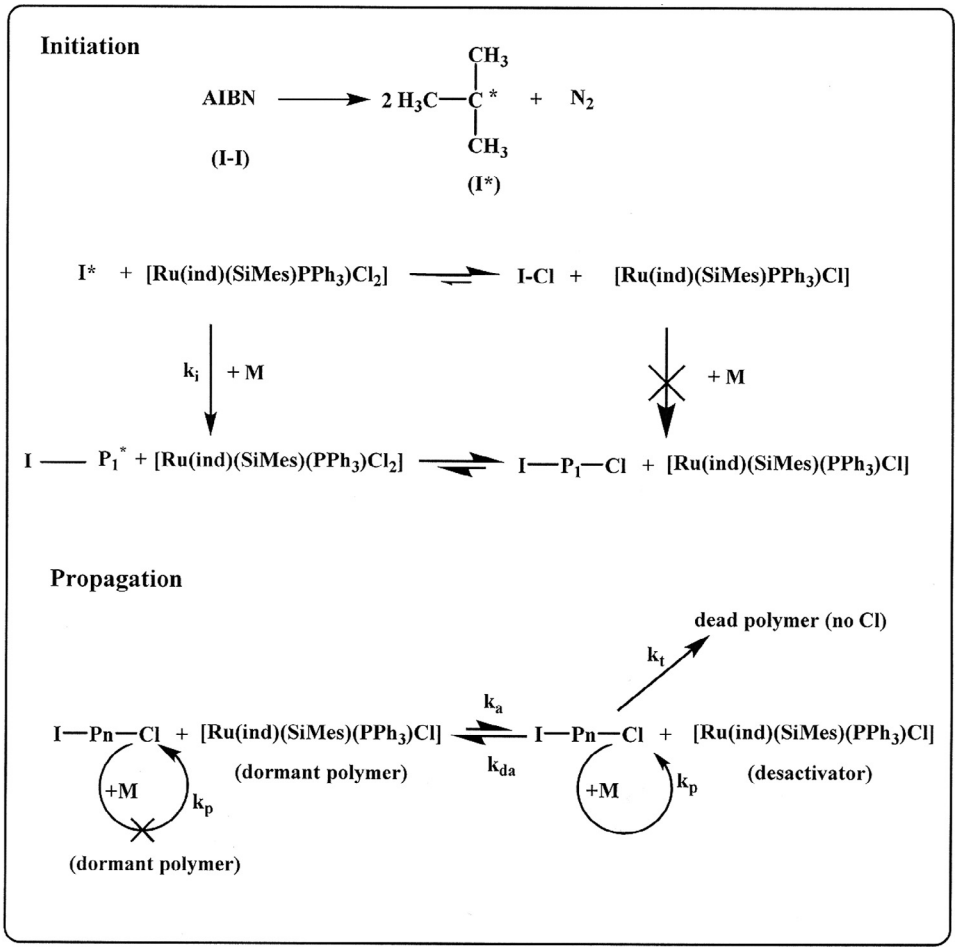

Scheme 3 Proposed mechanism of the polymerization of MMA involving the AIBN/M_{20} initiating system.

The treatment of the experimental data of Table 7 using Eq. (5) revealed in Fig. 6 a straight line passing through the origin.

This finding seems supports the hypothesis of a permanent quasi-stationary regime where the polymerization proceeds with an approximately constant number of active species for the duration of the reaction, thereby considerably limiting the possibility of transfer reactions. However, this theory is only true for perfectly living systems, not in a radical system as here. In our case, there always exist termination and by this way not a perfectly living system is involved. The straight line still observed in a system with a non-zero k_t is due to the diffusional limitations on termination (k_t goes to zero value in the end). This fact reduced the relevance of k_t and changes the curvature of the logarithmic plot to linear. This phenomenon is widely explained by D'Hooge et al. (2012). The positioning by nonlinear regression has led us to the K_p^{app} value of $7.86 \times 10^{-5}\ s^{-1}$ with the experimental errors estimated at 95% confidence limits. These results also highlight that the propagation obeys to a first order rate law with regard to the concentration of monomer. These data confirm the previous results concerning the superior efficacy of the initiating system involving the M_{20} complex. Accordingly, the propagation rate, R_p, under these conditions, can be represented by the following relationship

$$R_p = 7.86 \times 10^{-5}\ [\text{MMA}] \quad (7)$$

The results achieved so far are, however rather limited to rigorously explain the control mechanism of the polymerization of MMA, because of the lack of supplementary analysis. However, in this case, we can always propose a mechanism as that presented in Scheme 3 inspired from those proposed by Chen and Qiu involved the AIBN/$FeCl_3$/PPh_3 initiating system (Chen and Qiu, 2000), Matyjaszewski et al. involved a conventional radical initiator (Wang and Matyjaszewski, 1995) and Teyssié et al. involved $NiBr_2(PPh_3)_2$ as catalyst (Moineau et al., 1998).

According to this mechanism, in the initiation step, the primary radical R^* or the active species in the propagating chain R-P_1 abstracts an atom of Cl from the highly oxidized transition-metal of the Ru(ind)(SIMes)(PPh_3)Cl_2 species and the dormant species R-Cl or R-P_1-Cl. The subsequent propagating steps then follow conventional ATRP.

3.6. Influence of the temperature

The effect of the polymerization temperature on the polymer yield, molecular weight and PDI was examined between 50 and 90 °C and the results are plotted in Fig. 7. As shown in these curve profiles, the average molecular weight increased with temperature and reached a maximum at 80 °C. Furthermore, the polymer yield grows quasi-linearly as the tempera-

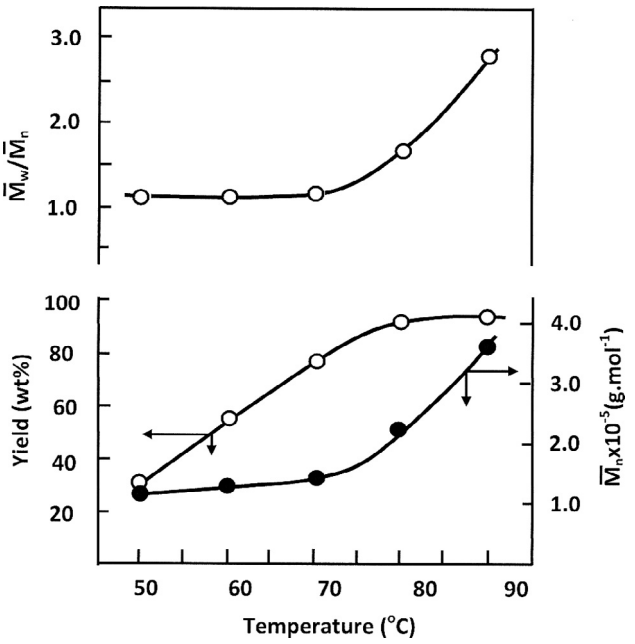

Fig. 7 Effect of the temperature on the yield, the average number molecular weight and $\overline{M}_w/\overline{M}_n$ of the PMMA obtained. The experimental conditions were: solvent: 1,4-dioxane; aging temperature: 70 °C; aging time: 5 min; polymerization time: 6 h; [AIBN] = 0.1 mg ($1.22 \cdot 10^{-3}$ mol L^{-1}); [MMA] = 2.48 g (4.68 mol L^{-1}); [AIBN]/[Ru] = 1.

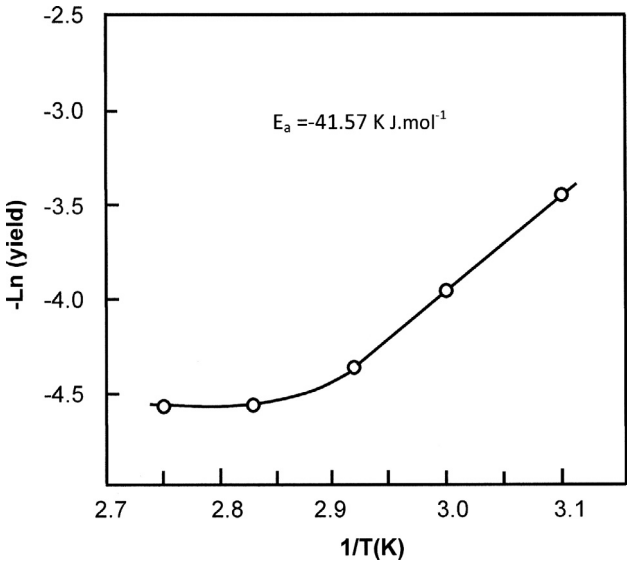

Fig. 8 Arrhenius curve indicating the variation of Log(yield) of PMMA versus T(K)$^{-1}$. The experimental conditions were: solvent: 1,4-dioxane; aging temperature: 70 °C; aging time: 5 min; polymerization time: 6 h; [AIBN] = 0.1 mg ($1.22 \cdot 10^{-3}$ mol L^{-1}); [MMA] = 2.48 g (4.68 mol L^{-1}); [AIBN]/[Ru] = 1.

ture remains inferior to 70 °C followed by a dramatic linear increase. While presently we lack the information to rigorously explain these experimental results, we can propose that the increase of the molecular weight in the examined temperature range, and the stabilization of the yield beyond 70 °C might be related to a progressive deactivation of the polymerization sites when the increased. However, the induction period was observed for polymerization carried out at 70–90 °C. It is also apparent that the higher the reaction temperature, the shorter the induction period, as might be expected. During the early stages of polymerizations at temperature between 60 and 80 °C, the primary radicals generated from AIBN seems to react completely with [(SiMes)Ru(PPh$_3$)(Ind)Cl$_2$] complex to form new active species responsible for the production well-defined polymers characterized by narrow PDI. The slight increase of the molecular weight distribution observed in up of this same figure at above 80 °C is probably due to some thermal polymerizations via traditional radical polymerization caused by an eventual strongly non isothermal reaction, in addition to that initiated by the AIBN/M$_{20}$ system which involves most of the monomer. Indeed, the yields are lower for higher initial monomer concentrations and the average molar masses higher there is a stronger effect of diffusional limitations probably.

It is well known that the free radical polymerization leads to uncontrolled polymer stereo-structure due to planarity of the propagating active center (Habaue and Okamoto, 2001, Isobe et al., 2000, Farina, 1981). Varying the temperature has a limited effect on the polymer tacticity. In general, lowering the polymerization temperature favors syndiotacticity (Gong et al., 2006). In this investigation, it was found that the AIBN/M$_{20}$ initiating system is capable to initiate CRP of MMA in a wide temperature range (50–90 °C) and leads not only to a controlled molecular weight but also a relatively regular stereo-structure. Table 8 summaries the *mm*, *mr*, *rr* triads contents in the PMMA structure obtained from the polymerization reaction in the presence of AIBN/M$_{20}$ system at different temperatures. Increasing the temperature from 50 to 90 °C leads to a decrease in the *rr* (syndiotactic) triads (from 78 to

Table 8 Effect of the polymerization temperature on the PMMA tacticity.

Experiment	Temperature (°C)	Triad tacticity (%)		
		mm	*mr*	*rr*
1	50	3	19	78
2	60	4	21	75
3	70	4	23	73
4	80	6	33	61
5	90	9	39	52

Experimental conditions: Solvent: 1,4-dioxane; aging temperature: 70 °C; aging time: 5 min; [AIBN]/[Ru] = 1; [AIBN] = 0.1 mg L^{-1} ($1.22 \cdot 10^{-3}$ mol L^{-1}); [MMA] = 2.35 g (4.68 mol L^{-1}); polymerization temperature: 70 °C.

Table 9 Effect of the nature of solvent on the results of the polymerization of MMA.

Experiment	Solvent	$\delta(MPa^{1/2})$	$\Delta\ \delta(MPa^{1/2})$	Yield (wt%)	$\overline{M}_n \times 10^{-5}$ (g mol^{-1})	$\overline{M}_w \times 10^{-5}$ (g mol^{-1})	$\frac{\overline{M}_w}{\overline{M}_n}$
1	Bulk	–	–	78.82	1.32	1.45	1.10
2	1,4-Dioxane	20.5	1.5	56.22	1.04	1.13	1.09
4	Toluene	18.3	0.7	58.20	1.12	1.27	1.13
5	2-Butanone	19.3	0.3	74.00	1.40	1.54	1.10
3	Chloroform	19.0	0	82.27	1.54	5.17	3.36

Preparation conditions: aging temperature: 70 °C; aging time: 5 min; [AIBN]/[Ru] = 1; [AIBN] = 0.1 mg L^{-1} ($1.22 \cdot 10^{-3}$ mol L^{-1}); [MMA] = 2.35 g (4.68 mol L^{-1}); polymerization time: 3 h; polymerization temperature: 70 °C.

Table 10 Effect of nature of solvent on the PMMA tacticity.

Experiment	Solvent	Triad tacticity (%)		
		mm	*mr*	*rr*
1	Bulk	3	19	78
2	1,4-Dioxane	4	23	73
3	$CHCl_3$	4	20	76
4	Toluene	6	17	77
5	2-Butanone	9	16	75

Preparation conditions: aging temperature: 70 °C; aging time: 5 min; [AIBN]/[Ru] = 1; [AIBN] = 0.1 mg L^{-1} ($1.22 \cdot 10^{-3}$ mol L^{-1}); [MMA] = 2.35 g (4.68 mol L^{-1}); polymerization time: 3 h; polymerization temperature: 70 °C.

52%), While, the mr triads increased from 19 to 39%. Similar results were have been noted by (Miura et al., 2006) using the copper-mediated ATRP in 1,1,1,3,3,3-hexafluoro-2-propanol (HFIP).

According to Smith and Coote (2013), the syndiotactic tendency of PMMA is attributed to the steric repulsion that exists between the bulky ester side chains in which the helical chains are favored leading to an alternative arrangement minimizing the steric repulsion.

The effective activation energy, E_a, was obtained from the slope of the linear portion in the Arrhenius plot (Ln(yield) versus T^{-1}, Fig. 8) to be 41.57 kJ mol^{-1}. This value is approximately 2.5 times inferior to that determined by Bulgakova (Bulgakova et al., 2011a) using AIBN combined with iron (III) chloride in dimethylformamide occurred without 1-acetyl-2-phenylhydrazine and two times higher than that obtained by pure radical polymerization initiated by AIBN initiator (Young and Lovell, 2011).

3.7. Effect of solvent

Polymerization of MMA was also been carried out in different solvents namely toluene, chloroform, 1,4-dioxane and 2-butanone. According to the experimental data in Table 9, a slightly difference is observed between the results obtained in the 1,4-dioxane (yield = 56.22%, $M_n = 1.04 \times 10^5$ g mol^{-1}, PDI = 1.09) and the toluene (yield = 58.20%, $M_n = 1.12 \times 10^5$ g mol^{-1}, PDI = 1.13). While, the higher yield was obtained in the chloroform with 82.27% of PMMA with the higher PDI (3.36). Practically no difference was revealed between the polymerization results obtained with 2-butanone with regard to those obtained in the bulk indicating that this solvent no affects the polymerization process.

The PDI barely changed when varying the nature of solvent (1.03–1.15). The comparable values of the Henssen solubility parameters, δ, of these solvents taken from the literature (Brandrup et al., 1999) are presented in Table 9. These data reveal that the polymerization results obtained under these conditions are closely linked to the solubility of the PMMA macro-radicals in the solvent. So, the polymer yield increased when their solubility difference between PMMA and that of the solvent approaches zero, in other words, when the solubility of the macro-radical increases. Concerning the stereo-structure of PMMA determinate by ^{1}H NMR spectroscopy (Table 10), the *rr* (syndiotactic sterio-structure) triad of PMMA remains a major feature (75.3–78.2%) and it is not significantly affected by the presence or nature of solvent. The

Table 11 Comparison of yields and molecular weights between some vinylic polymers synthesized in presence of AIBN alone and those obtained by the AIBN/M_{20} system in the same conditions.

Polymer	AIBN[a]				AIBN/M_{20}[b]			
	Yield (wt%)	$M_n x10^{-5}$ (g mol^{-1})	$M_w x10^{-5}$ (g mol^{-1})	$\frac{\overline{M}_w}{\overline{M}_n}$	Yield (wt%)	$M_n x10^{-4}$ (g mol^{-1})	$M_w x10^{-4}$ (g mol^{-1})	$\frac{\overline{M}_w}{\overline{M}_n}$
PMA	87.27	3.5	15.2	4.35	78.55	23.0	27.1	1.18
PMMA	93.78	2.7	8.9	3.28	74.22	14.0	15.4	1.10
PEMA	90.34	3.4	10.5	3.13	68.06	18.0	18.9	1.05
PBMA	97.23	3.2	8.5	2.67	78.00	13.0	14.6	1.12
PAM	86.65	2.9	9.0	3.12	89.36	27.0	31.1	1.15
PS	92.06	9.8	41.5	4.23	75.12	9.21	11.1	1.20

Experimental conditions: Solvent, a, b) 2-Butanone; b) aging temperature: 70 °C; b) aging time: 5 min; b) [AIBN]/[Ru] = 1; a, b) [AIBN] = 0.1 mg L^{-1} ($1.22 \cdot 10^{-3}$ mol L^{-1}); a, b) [MMA] = 2.35 g (4.68 mol L^{-1}); a, b) polymerization temperature: 70 °C.

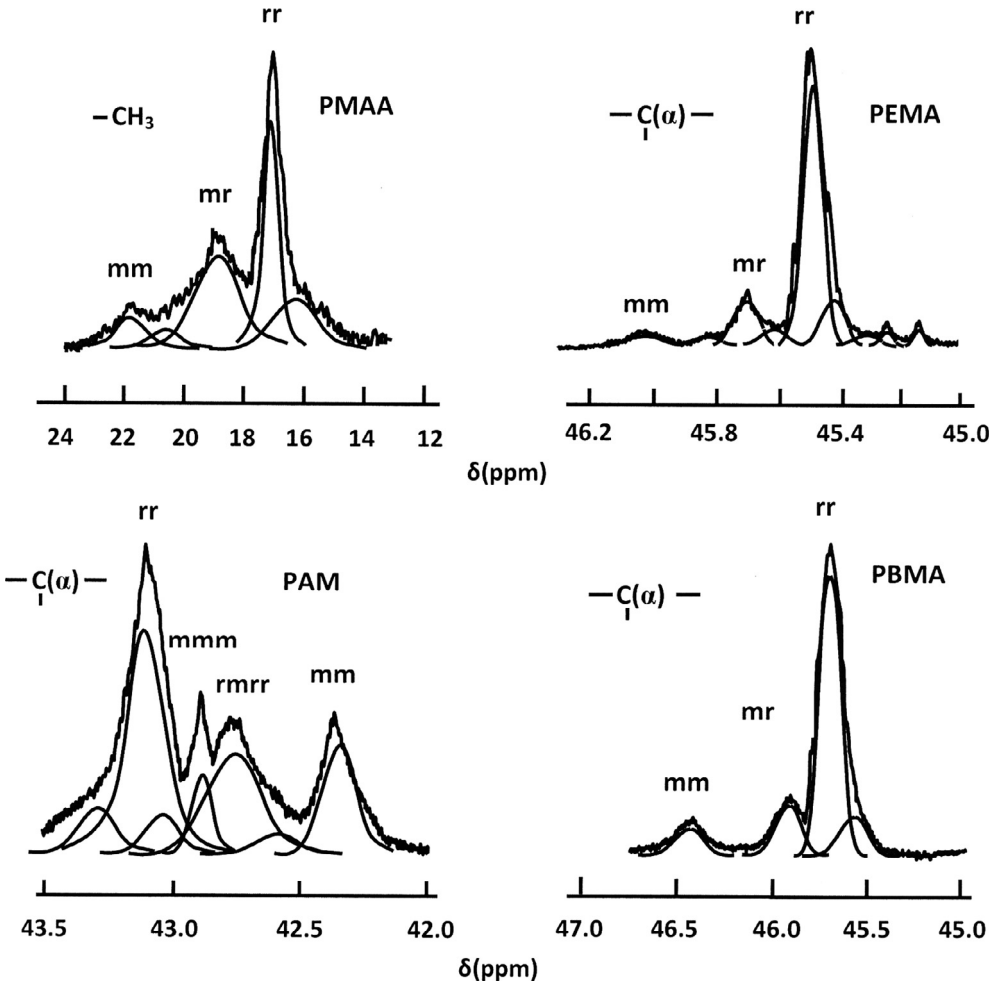

Fig. 9 Deconvolution of the ^{13}CNMR spectra of PMAA in (12–24 ppm), PEMA in (45–46 ppm), PAM in (42–43.5 ppm) and PBMA (45.5–47.0 ppm) ranges via Lorentzian peaks.

results reported by Smith and Coote (2013) on the polymerization of MMA using DMSO, DMF, THF, acetonitrile and acetone as solvents attribute the triad fractions of PMMA obtained to the deviations from the Bernoulli model, implying that the antepenultimate unit affects the propagation.

3.8. Polymerization of some vinylic monomers

The optimum conditions we determined for the polymerization of MMA were applied to the reactions of EMA, BMA, MAA, AM and St. The results are compared with those obtained by AIBN alone under the same conditions, as tabulated in Table 11. In general, the PDI of the polymers obtained by the AIBN/M_{20} initiating system drops at about three times compared with those obtained by AIBN alone, while the yield and the average molecular weight were decreased. This finding can be due to a high viscosity of the media observed during the polymerization process, which is likely caused by a complex formation between the monomer and M_{20} compared with that using the AIBN alone. Indeed, it is well-known that an increase in the medium viscosity reduces the propagation rate of the polymerization. thus reducing the chains growth.

The stereo-structure of these polymers synthesized by the AIBN/M_{20} initiating system, determined by ^{13}CNMR method, is shown in Fig. 9. The deconvolution of the broad peaks in other characteristic peaks assigned to the *rr*, *rm* and *mm* triads reveals the stereo-structures given in Table 12. The AIBN/M_{20} system guides the polymerization of methacrylate esters toward a stereo-structure that is mainly syndiotactic. On the other hand, practically no change in the stereo-structure of poly(methacrylic acid)(PMA) was observed upon the addition of M_{20} complex to the AIBN initiator. Unlike the case of PMA, the combination of AIBN with M_{20} changes the stereo-structure of the poly(acrylamide)(PAM) from the *rr*, *rm* and *mm* triads to one rich in *rr* and *mm* triads, while it changes the stereo-structure of PSt from triads rich in *rr* and *rm* to ones rich in *rr* and *mm*.

4. Conclusion

AIBN combined with M_{20} is an effective initiating system for the controlled radical polymerization of MMA. When this initiating system was used to polymerize MMA in homogeneous solutions, the resultant PMMA had a high syndiotactic con-

Table 12 Comparison of stereo-structures and glass transition temperatures between some vinylic polymers synthesized in presence of AIBN alone and those obtained by the AIBN/M_{20} system in the same conditions.

Polymer	AIBN[a]				AIBN/M_{20}[b]			
	Triadrr (%)	Triadrm (%)	Triadmm (%)	T_g (°C)	Triadrr (%)	Triadrm (%)	Triadmm (%)	T_g (°C)
PMA	54	39	7	228	43	43	14	205
PMMA	56	38	6	110	75	16	9	125
PEMA	57	35	8	51	84	13	3	120
PBMA	62	33	5	22	87	7	5	88
PAM	35	43	22	168	50	7	43	161
PSt	37	52	11	100	56	4	40	105

Experimental conditions: Solvent, a, b) 2-Butanone; b) aging temperature: 70 °C; b) aging time,: 5 min; b) [AIBN]/[Ru] = 1; a, b) [AIBN] = 0.1 mg L^{-1} ($1.22 \cdot 10^{-3}$ mol L^{-1}); a, b) [MMA] = 2.35 g (4.68 mol L^{-1}); a, b) polymerization temperature: 70 °C.

tent (61–78%) very difficult to obtain at time by the different CRP methods. The polymerization of MMA was examined under various aging time of the initiating system, concentration of monomer, AIBN/M_{20} molar ratio, polymerization time, temperature of polymerization and nature of the solvent. The results revealed that the polymers were characterized by relatively high molecular weights (0.72×10^5–5.12×10^5 g moL^{-1}), narrow molecular distribution (1.08–1.47), and rich syndiotactic microstructure. The best performance of the AIBN/M_{20} initiating system was reached under the aging time of 5 min, concentration of MMA of 4.8 mol L^{-1}, AIBN/M_{20} ratio 1:1, polymerization time of 6 h, polymerization temperature of 70 °C and 2-butanone as solvent. The kinetic data indicated first order kinetics with respect to concentration of monomer, with a rate constant value of 7.86×10^{-5} s^{-1}. This finding supports the hypothesis of the permanent quasi-stationary regime, indicating that the polymerization proceeds with an approximately constant number of active species for the duration of the reaction, in which the propagation centers disappear and form at the same rates. The effective activation energy (41.6 kJ mol^{-1}) is twice that found for pure radical polymerization of MMA initiated by AIBN. Applying this initiating system to the polymerization of other vinylic monomers produced polymers with PDI value about three times lower compared with those obtained by AIBN alone, while the yield and the average molecular weight decreased. It was also found It was also found that, the produced ester polymers are mainly syndiotactic accept that of PMA in which the stereo-structure remains unchanged. The combination of AIBN with M_{20} changes the stereo-structure of PAM from the *rr*, *rm* and *mm* triads to one rich *rr* and *mm* triads. On the other hand, the same initiating system changes the stereo-structure of PSt from triads rich in *rr* and *rm* to a triads rich in *rr* and *mm*.

Acknowledgment

The authors extend their sincere appreciations to the Deanship of Scientific Research at King Saud University for funding this work through research group NO (RGP-1438-040).

References

Agapov, A.L., Sokolov, A.P., 2009. Macromolecules 42, 2877–2878.
Al-Majid, A.M., Shamsan, W.S., Al-Odayn, A.-B.M., Nahra, F., Aouak, T., Nolan, S.P., 2017. Des. Monomers Polym. 20, 167–176.
Ando, T., Kato, M., Kamigaito, M., Sawamoto, M., 1996. Macromolecules 29, 1070–1072.
Arslan, H. Block, 2012. Graft Copolymerization by Controlled/Living Radical Polymerization Methods, Materials Science, plymers. book Edited by De Souza Gomes, A. September 12, 2012.
Bao, F., Feng, L., Gao, J., Tan, Z., Xing, B., Ma, R., Yan, C., 2010. PloS one 5, e13629.
Bedri, B., Cikilmazkaya, M., Tunca, U., Hizal, G., 2003. Des. Monomers Polym. 6, 299–307.
Beevers, R.B., White, E.F.T., 1960. Trans. Faraday Soc. 56, 1529–1534.
Blanchard, L.P., Hess, J., Malhotr, S.L., 1974. Can. J. Chem. 52, 3170–3175.
Brandrup, J., Immergut, E., Grulke, E., 1999. Willey, New York, 282.
Bulgakova, S., Tumakova, E., Zhizhikina, A., Zaitsev, S., Kurushina, L., Semchikov, Y.D., 2011a. Polym. Sci. Series B 53, 57–63.
Bulgakova, S., Volgutova, E., Kiseleva, E., Khokhlova, I., Semchikov, Y.D., 2011b. Polym. Sci. Series B 53, 563–567.
Chen, G., Zhu, X., Cheng, Z., Wenjian, X., Lu, J., 2004. Radiat. Phys. Chem. 69, 129–135.
Chen, X.P., Qiu, K.Y., 2000. Polym. Int. 49, 1529–1533.
De Clercq, B., Verpoort, F., 2003. Polym. Bull. 50, 153–160.
De Frëmont, P., Clavier, H., Montembault, V., Fontaine, L., Nolan, S. P., 2008. J. Mol. Catal. A: Chem. 283, 108–113.
D'Hooge, D.R., Konkolewicz, D., Reyniers, M.F., Marin, G.B., Matyjaszewski, K., 2012. Kinetic modeling of ICAR ATRP. Macromol. Theory Simul. 21, 52–69.
Dragutan, V., Dragutan, I., Verpoort, F., 2005. Platin. Met. Rev. 49, 33–40.
Farina, M., 1981. Macromol. Chem. Phys. 4, 21–35.
Fox, T.G., Flory, P.J., 1950. J. Appl. Phys. 21, 581–591.
Gong, S., Hongyang Ma, H., Wan, X., 2006. Polym. Int. 55, 1420–1425.
Goto, A., Ohtsuki, A., Ohfuji, H., Tanishima, M., Hironori Kaji, H., 2013. J. Am. Chem. Soc. 135, 11131–11139.
Goto, A., Hirai, N., Wakada, T., Nagasawa, K., Tsujii, Y., Fukuda, T., 2008. Macromolecules 41, 6261–6264.
Habaue, S., Okamoto, Y., 2001. Chem. Record 1, 46–52.
Hiraki, K., Kaneko, S., Hirai, H., 1971. Polym. J. 2, 225–230.
Isobe, Y., Yamada, K., Nakano, T., Okamoto, Y., 2000. J. Polym. Sci., Part A: Polym. Chem. 38, 4693–4703.
Jafarpour, L., Schanz, H.-J., Stevens, E.D., Nolan, S.P., 1999. Organometallics 18, 5416–5419.
Jiang, W., Yang, W., Zeng, X., Fu, S., 2004. J. Polym. Sci., Part A: Polym. Chem. 42, 733–741.
Kato, M., Kamigaito, M., Sawamoto, M., Higashimura, T., 1995. Macromolecules 28, 1721–1723.
Le, D., Morandi, G., Legoupy, S., Pascual, S., Montembault, V., Fontaine, L., 2013. Eur. Polym. J. 49, 972–983.

Kuroda, T., Taniyama, T., Kitayama, Y., Okubo, M., 2015. Macromolecules 48, 2473–2479.
Lin, F., Li, Q., Jiang, D., Yu, X., Li, L., 2009. Iranian Polym. J. (English Edition) 18, 561–568.
Liu, X.-H., Li, H.-N., Zhang, F.-J., Xie, S., Liu, Z.-J., Li, Y.-G., 2015. Chin. J. Polym. Sci. 33, 362–370.
Matyjaszewski, K., Xia, J., 2001. Chem. Rev. 101, 2921–2990.
Miura, Y., Satoh, T., Narumi, A., Nishizawa, O., Okamoto, Y., Kakuchi, T., 2006. J. Polym. Sci., Part A: Polym. Chem. 44, 1436–1446.
Moad, G., Solomon, D.H., Spurling, T.H., Johns, S.R., Willing, R.I., 1986. Aust. J. Chem. 39, 43–50.
Moineau, G., Dubois, Ph., Jérome, R., Senninger, T., Teyssié, Ph., 1998. Macromolecules 31, 545–547.
Monsaert, S., De Canck, E., Drozdzak, R., Van Der Voort, P., Hendrickx, P.M., Martins, J.C., Verpoort, F., 2010. Green Metathesis Chemistry. Springer, pp. 31–38.
Pan, J.-L., Li, Z., Zhang, L.-F., Cheng, Z.-P., Zhu, X.-L., 2014. Chin. J. Polym. Sci. 32, 1010–1018.
Semsarzadeh, M.A., Daronkola, M.R.R., 2006. Iran. Polym. J. 15, 829–839.
Siegwart, D.J., Oh, J.K., Matyjaszewski, K., 2012. Progr. Polym. Sci. 37, 18–37.
Simal, F., Sebille, S., Hallet, L., Demonceau, A., Noels, A.F., 2000. Macromol. Symposia 161, 73–86.
Smirnov, B., Plotnikov, V., Ozerkovskii, B., Roshchupkin, V., Yenikolopyan, N., 1981. Polym. Sci. USSR 23, 2807–2816.
Smirnov, V., 1990. Polym. Sci. USSR 32, 524–532.
Smith, L.M., Coote, M.L., 2013. J. Polym. Sci., Part A: Polym. Chem. 51, 3351–3358.
Thompson, E.V., 1966. J. Polym. Sci. Part A-2: Polym. Phys. 4, 199–208.
Xia, J., Matyjaszewski, K., 1997. Macromolecules 30, 7692–7696.
Xiao, Q., Zhang, X., Yi, J., Wang, X., Zhang, H., 2008. Iran. Polym. J. 17, 781–790.
Young, R.J., Lovell, P.A., 2011. Introduction to Polymers. CRC Press.
Wang, J.S., Matyjaszewski, K., 1995. Macromolecules 28, 7572–7573.